BBA - Molecular and Cell Biology of Lipids 1865 (2020) 158640

Contents lists available at ScienceDirect

BBA - Molecular and Cell Biology of Lipids

journal homepage: www.elsevier.com/locate/bbalip

Dysregulation of microRNA-125a contributes to obesity-associated insulin resistance and dysregulates lipid metabolism in mice

Rui Liu[a], Meina Wang[a], Enjie Li[a], Yang Yang[a], Jiaxin Li[a], Siyu Chen[b], Wen-Jun Shen[c,d], Salman Azhar[c,d], Zhigang Guo[a], Zhigang Hu[a,*]

[a] Jiangsu Key Laboratory for Molecular and Medical Biotechnology, College of Life Sciences, Nanjing Normal University, 1 WenYuan Road, Nanjing 210023, China
[b] School of Life Science and Technology, China Pharmaceutical University, Nanjing 211198, China
[c] Geriatric Research, Education and Clinical Center, VA Palo Alto Health Care System, Palo Alto, CA 94304, USA
[d] Division of Endocrinology, Stanford University School of Medicine, Palo Alto, CA 94304, USA

ARTICLE INFO

Keywords:
microRNA-125a
Insulin sensitivity
Lipids metabolism
Fatty acid

ABSTRACT

Obesity is associated with an increased risk of developing insulin resistance (IR) and type 2 diabetes (T2D). A diverse group of factors including miRNA has been implicated in the pathogenesis of these two metabolic conditions, although underlying molecular mechanisms involved are not well defined. Here, we provide evidence that hepatic miR-125a levels are diminished in both genetic as well as dietary mouse models of obesity. Overexpression of miR-125a enhanced insulin signaling and attenuated cellular lipid accumulation in HepG2 cells and Hepa1–6 cells. Likewise, treatment of mice with ago-miR-125a increased insulin sensitivity, similar to overexpression of miR-125a, whereas treatment of mice with antago-miR-125a blunted the insulin sensitivity. Furthermore, overexpression of miR-125a in mice previously fed a high-fat diet (HFD), significantly improved insulin sensitivity, and attenuated obesity-linked hepatic steatosis and hepatocyte lipid accumulation. In addition, we show that ELOVL fatty acid elongase 6 (*Elovl6*) is a direct target of miR-125a, and participates in miR-125a mediated regulation of insulin sensitivity and lipid metabolism. These data led us to conclude that dysregulated miR-125a expression augments the development of obesity-induced IR and that miR-125a might serve as a therapeutic target for the development of new drug(s) in the clinical management of metabolic diseases.

1. Introduction

Obesity, an inflammatory condition [1], is a worldwide health problem [2] and increases the risk of cardiovascular disease (CVD) [3], metabolic syndrome (MetS) [4], T2D [5], and nonalcoholic fatty liver disease (NAFLD) [6]. One hallmark of obesity is the alteration in metabolic and cellular functions as a result of dysregulated lipid and glucose metabolism, insulin resistance and chronic low-grade systemic inflammation [7]. Although, many genetic, metabolic and physiological factors have been implicated in the pathogenesis of dyslipidemia and insulin resistance [8–10], however, the underlying mechanism(s) of these obesity-induced metabolic alterations remain largely unexplored.

MicroRNAs (miRNAs) is a class of small, non-coding RNAs (~22 nucleotides) that modulate gene expression post-transcriptionally by targeting mRNA 3′-untranslated regions (3′-UTRs) through base pairing [11,12]. MiRNAs have been shown to regulate numerous diverse biological processes such as development, cell differentiation, cell proliferation, lipogenesis, gluconeogenesis and carcinogenesis [13–15]. Recently, several studies have identified miRNAs including miR-122, miR-143, miR-130a-3p, miR-26a, miR-802, miR-103 and miR107 that are critically involved in metabolic homeostasis [14,16–20]. Moreover, it has been reported that the expression profile of different types of miRNAs was altered in obese mouse liver, adipose tissue and other tissues [11,19–23]. In addition, several obesity-related miRNAs have been identified that can serve as a novel metabolic biomarkers in obese subjects [24,25]. Overall, these findings suggest that miRNAs play a central role in cellular metabolic homeostasis and may serve as promising therapeutic targets in the development of new therapies to treat metabolic disorders.

MiR-125a, which is highly conserved throughout diverse species from nematode to humans, has been implicated in a variety of pathophysiological processes including cell proliferation, apoptosis, Inflammation, carcinomas and other diseases [26–29]. Although miR-125b (the miR-125a homolog) was reported as oncogene in several types of cancer [27,30], other studies have shown that miR-125a functions as tumor-suppressor in several types of cancer such as ovarian

* Corresponding author.
E-mail address: huzg_2000@126.com (Z. Hu).

https://doi.org/10.1016/j.bbalip.2020.158640
Received 24 September 2019; Received in revised form 27 December 2019; Accepted 23 January 2020
Available online 25 January 2020
1388-1981/

cancer, bladder cancer, breast cancer, hepatocellular carcinoma, melanoma, cutaneous squamous cell carcinoma and osteosarcoma [27]. In addition, it has been reported that the functional expression of miR-125a is downregulated in several human cancers including hepatocellular carcinoma, non-small cell lung cancer, neuroblastoma, medulloblastoma and glioblastoma [26,31,32].

We previously demonstrated that miR-125a is critically involved in the regulation of cholesterol uptake and steroidogenesis by targeting high-density lipoprotein receptor, scavenger receptor class B, type 1 (SR-B1) [15]. Interestingly, up-regulation of miRNA-125a expression has also been demonstrated in livers of a spontaneous rat model of Type 2 Diabetes [33]. In contrast, another study reported reduced expression of miR-125a in adipose tissue of mice fed a high fat diet as well as in experimentally-induced insulin resistant 3T3-L1 adipocytes (IR-3T3-L1) [34]. In addition, miR-125a expression is also downregulated in adipose tissue of obese subjects [34]. These results suggest that miR-125a may be associated with metabolic homeostasis and insulin sensitivity, although the extent of its involvement and the exact mechanism(s) by which miR-125a impacts lipid metabolism and insulin sensitivity are not well delineated at present.

In this study, we analyzed the miRNA expression profiles of liver from mice fed a high-fat diet (high fat diet induced obese [DIO] C57BL/6J mice) and found that the expression of miR-125a was significantly reduced in livers of DIO mice. Likewise, we also observed the down-regulation of miR-125a expression in obese leptin-deficient, *ob/ob* mice. Overexpression of miR-125a markedly attenuated lipid accumulation and improved insulin resistance both under in vitro and in vivo conditions. Our study identified key regulatory functions of miR-125a that participate in the regulation of insulin sensitivity and lipid metabolism.

2. Methods

2.1. Animals

All animal experiments were performed in accordance with the Guide for the Care and Use of Laboratory Animals published by the National Institutes of Health (NIH publication 85-23, revised in 1996) and the procedures approved by the Laboratory Animal Care Committee at Nanjing Normal University (Permit 2090658, issued 20 April 2008). Male C57/BL6 mice and *ob/ob* mice were purchased from the Model Animal Research Center of Nanjing University (Nanjing, Jiangsu, China). Mice were housed on a 12-h light/dark cycle at 25 °C with either normal laboratory chow diet (CD) or high fat diet (HFD) (D12492; Research Diets, New Brunswick, NJ). Mice body weights were monitored every week. For HFD studies, WT mice were fed HFD starting at the age of 8 weeks, and the maintained on the diet for an additional 8 weeks. For miRNA injection experiments, mice were administrated intravenously by tail vein injection 50 mg/kg 5′ Chol-labeled miR-125a agomir (Ago-miR-125a), miR-125a antagomir (Antago-miR-125a) or scrambled negative control ago-miRNA (miR-NC) (Guangzhou RiboBio Co., Ltd., China) respectively twice on days 1 and 3 in the14th week of HFD feeding (Fig. 4A).

2.2. Glucose and insulin tolerance tests

Glucose tolerance test (GTT) was performed with 16 h-fasted mice as previously described [35]. Each animal received an intraperitoneal injection of 1 g/kg glucose (Sigma-Aldrich, St. Louis, MO, USA) in sterile saline. Blood glucose levels were measured at 0, 15, 30, 60, 90, and 120 min after the injection. For insulin tolerance test (ITT), mice were injected intraperitoneally with an insulin solution (Sigma-Aldrich) at 0.5 U/kg after 4 h of fasting. Blood glucose levels were monitored at 0, 15, 30, 45, 60, 90, and 120 min after the injection.

2.3. Insulin signaling

In vivo insulin treatment (stimulation) and analysis of insulin signaling were performed as described previously, with minor modifications [17]. Briefly, After 6 h of fasting, mice were anaesthetized and the abdominal cavity of the mice was opened to inject with insulin at a dose of 2 units/kg/control mouse or 5 units/kg/HFD mouse via the portal vein. Samples of liver were collected 2 and 5 min after insulin injection respectively, and tissue extracts were prepared for western blot analysis.

2.4. Plasmid

The luciferase-UTR reporter constructs were generated by introducing the DNA fragments of 3′-untranslated regions (UTRs) from mouse ELOVL6 containing potential miR-125a-5p binding sites into the pMIR-report luciferase vector with CMV promoter (Applied Biosystems, CA), as previously described [11,12]. The forward and reverse primers contained Hind III and Spe I recognition sites at the 5′ end of the primers, respectively. Mutagenesis of the miR-125a binding sites was carried out according to the instructions supplied by the manufacture of the QuikChange II site-directed mutagenesis kit (Stratagene, La Jolla, CA). The inserted fragment was confirmed by sequencing. All primers for plasmid constructs are listed in Supplementary Table 1. MiR-125a mimics and inhibitors for cell transfection were purchased from RiboBio (Guangzhou, China).

2.5. Cell culture, treatment and transfection

Mouse Hepa1–6 cells, CHO-K1 cells and HepG2 cells were obtained from the Shanghai Institute of Cell Biology, Chinese Academy of Science. Cells were cultured in recommended medium supplemented with 10% fetal bovine serum and antibiotics. Most of the tissue culture supplies were purchased from Life Technologies™ through its Gibco® Cell Culture Media Division (Grand Island, NY). For transfection studies, cells were plated for 12-h prior to start of experiments and then Lipofectamine 3000 transfection reagent (Invitrogen, Carlsbad, CA, USA) was used for transient transfections according to manufacturer's instructions. Cells were transfected with miR-125a mimic, inhibitor or scrambled oligonucleotide for 48 h before carrying out the planed studies.

2.6. Microarray and quantitative RT-PCR (qRT-PCR) analysis of miRNA expression

Following feeding mice with HFD or control diet and/or miR-125a treatment, the animals were killed by cervical-dislocation. Liver samples were quickly removed, immediately snapped frozen in liquid nitrogen and stored frozen at −80 °C until analyzed. miRNA microarray was performed and analyzed by Oebiotech Company (Oebiotech, Shanghai, China) using Agilent Mouse miRNA arrays (8 ∗ 60K, Design ID:046065). For qRT-PCR, total RNA was extracted from cell lines using Trizol reagent (Invitrogen, USA) according to the manufacturer's protocol. To measure mRNA expression, total RNA (1 μg) samples from cells and livers were reverse-transcribed using SuperScript II reverse transcriptase (Invitrogen, Carlsbad, CA) and oligo(dt) primers. The resulting complementary cDNA samples were used for real-time quantitative PCR using qPCR kit (TAKARA Biotechnology, catalog no. RR420A) and gene-specific primers (Supplementary Table 1) on ABI StepOneplus system (Applied Biosystems, CA). Target mRNA expression was normalized to the 36B4 signal. Quantitative real-time PCR analyses of miRNA were performed with miRNA primer kit (RiboBio, Guangzhou, China). The relative miRNA expression of miRNAs was normalized to that of the internal control U6. Relative miRNA levels were calculated using the comparative threshold $2^{-\Delta\Delta Ct}$ method [15].

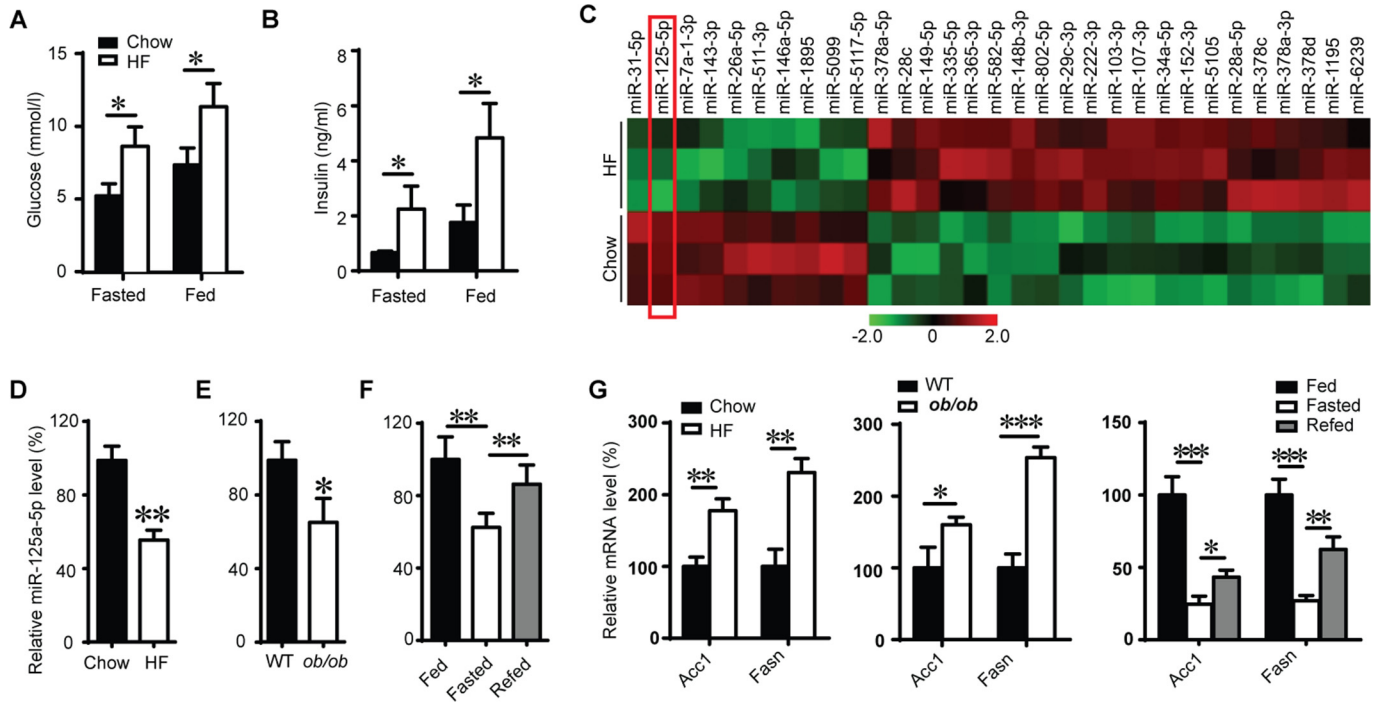

Fig. 1. MiR-125a expression is reduced in obese mice. (A) Plasma glucose levels and (B) insulin levels in C57BL/6J mice fed chow (n = 5) of HF diet (n = 5) for 8 weeks (*P < 0.05; by Student's *t*-test). (C) Microarray of miRNAs in the livers of C57BL/6J mice fed chow or HF diet. miR-125a was labeled in red frame. qRT-PCR detected relative miR-125a levels in livers of mice fed chow or HF diet (D), and in that of wide type (n = 3) or ob/ob mice (n = 3) (E) (*P < 0.05; **P < 0.01; by Student's *t*-test). (F) Relative miR-125a levels in livers of fasted (n = 4) or refed mice (n = 4) (**P < 0.01; by Student's *t*-test). (G) Relative mRNA levels of *Acc1* and *Fasn* in the same samples of D–F (*P < 0.05; **P < 0.01; ***P < 0.001; by Mann-Whitney test). Results are represented as means ± SEM.

2.7. Dual-luciferase assays

For the luciferase assay, CHO-K1 cells were co-transfected with internal control vector pRL-Renilla, different 3′ UTR pMIR-report constructs, and miR-125a mimic or scrambled oligonucleotide using Lipofectamine® 3000 transfection reagent (Invitrogen). Thirty-six hours after transfection, cells were harvested for activity assay using Dual-Glo Luciferase assay system (Promega) according to the manufacturer's instructions. Reporter activity was measured using an infinite f200 PRO microplate reader (Tecan Group Ltd., Männedorf, Switzerland). Renilla luciferase was used as an internal control.

2.8. Biochemical analyses

Blood samples were collected in nonheparinized tubes. After stewed at 4 °C, bloods were centrifuged at 3000*g* for 10 min. Sera samples were then collected and stored at −80 °C until further analysis. Triglyceride (TG) and total cholesterol (TC) levels in HepG2 cells, Hepa1–6 cells and murine livers were measured using commercially supplied kits (Jiancheng Institute of Biotechnology, Nanjing, China). Likewise, diacylglycerol (DAG) levels in HepG2 cells and Hepa1–6 cells were quantified using a commercial ELISA kit (SenBeiJia Biological Technology Co., Ltd., Nanjing, China).

2.9. Fatty acid composition of liver

The fatty acid composition was determined by gas chromatograph/mass spectrometric (GC/MS) using Agilent 7890A/5975C. The measurements were conducted by BioNovoGene Company (Suzhou, Jiangsu, China).

2.10. Western blot analysis

Cell or tissue extracts for Western blot analysis were first analyzed for protein content using BCA assay (Pierce Biotechnology, Rockford, IL, USA). For PKCε translocation assay, cell membrane proteins were extracted using a commercial kit (Beyotime Biotechnology, Shanghai, China). Subsequently, appropriate amount of samples (protein) were mixed with equal volumes of 5 × Laemmli sample buffer [120 mM Tris-HCl, pH 6.8, 2% SDS (w/v), 10% sucrose (w/v), and 1% 2-mercaptoethanol] and subjected to 12% SDS-PAGE. All western blot were performed using the standard procedure of the laboratory as previously descripted [36]. Antibodies used in Western blot analysis included anti–phospho-IRS^{S312} (1:1000), anti-IRS (1:1000), anti-phospho-IR^{Y1345} (1:1000), anti-ACC1 (1:1000), anti-FASN (1:1000), anti-PKCε, anti-Na^+/K^+-ATPase and anti-IR (1:1000) were obtained from ABclonal (Wuhan, China). Antibodies for anti–phospho-AKT^{S473} (1:1000) (9271, CST), anti-AKT (1:1000) (9272, CST), and anti-GAPDH (1:1000) (Bioworld technology co., Ltd., Nanjing, China), anti-ELOVL6 (1:1000), and TBB5 (1:1000) were purchased from (EnoGene Biotech Co., Ltd., New York, NY 10032, USA). Western blot gel bands were quantified using Image J program (https://imagej.nih.gov/ij).

2.11. Statistical analysis

Statistical analyses were performed using GraphPad Prism version 6.0. A P value of < 0.05 was considered as statistically significant. Data were analyzed for the assumption of normal distribution of data using the Kolmogorov-Smirnov test. If the data fitted to normal distribution (P > 0.05), statistical significance was determined by unpaired Student's *t*-test (two-tailed) between two groups. If the data did not fit to normal distribution (P < 0.05), Mann-Whitney test was used to analyze the data. The specific statistical tests used are indicated in the legends of each figure. *P < 0.05, **P < 0.01, ***P < 0.001. Data presented as mean ± SEM. GraphPad Prism was also used to create figures.

3. Results

3.1. Regulation of miR-125a expression

In order to identify miRNAs impacted by obesity and potentially contribute to the pathogenesis of obesity-associated complications, groups of C57BL/6J mice were fed with a normal chow diet (control diet) or HFD diet as described in the experimental section and used in various metabolic measurements. Feeding mice with HFD diet (diet-induce obese [DIO] mice) for eight weeks showed a significant body weight gain, elevated serum glucose and insulin levels as compared to mice fed a control diet (Fig. 1A, B and Supplementary Fig. 1A). Microarray analysis of microRNA was using liver samples from both control and diet-induced obese (DIO) mice (Fig. 1C and Supplementary Table 2) revealed that miR-125a was among the three most-down-regulated miRNAs in the livers of DIO mice. Moreover, miR-125a was one of the 31 predominant hepatic miRNAs, which showed statistical significance with high microarray signals (signal $>$ 500). The suppression of miR-125a expression in livers of DIO mice was further confirmed by performing qRT-PCR measurements (Fig. 1D). In addition, the expression levels of miR-125a were determined in the livers of the genetic obese leptin-deficient (*ob/ob*) mice. qRT-PCR analysis demonstrated that miR-125a expression was slightly reduced in livers of *ob/ob* mice as compared to lean mice (Fig. 1E). These results are in agreement with a previous report showing that *ob/ob* mice exhibit decreased hepatic expression of miR-125a [20]. We next determined the hepatic expression of miR-125a in mice, which were either fed ad libitum, fasted or fasted and refed. This analysis revealed a significant down-regulation of miR-125a in the liver of fasted mice but returned to normal levels in response to refeeding (Fig. 1F). The mRNA expression levels of key hepatic lipogenic genes, acetyl-CoA carboxylase 1 (*Acc1*) and fatty acid synthase (*Fasn*) were measured in RNA samples isolated from different groups of mice by qRT-PCR. Our data presented show that *Acc1* and *Fasn* were up-regulated in the livers of *ob/ob* and DIO mice, while both these genes were down-regulated after fasting and partially recovered with refeeding (Fig. 1G and Supplementary Fig. 1B–D).

3.2. MiR-125a regulates lipid accumulation and insulin sensitivity in vitro

To explore the role of miR-125a in the regulation of lipid metabolism and insulin sensitivity, miR-125a mimic were overexpressed ~1000 fold in HepG2 cells and hepa1–6 cells, while miR-125a levels were down-regulated ~40% by the inhibitor (Fig. 2A). As shown in Fig. 2B, C and D, TG, TC and DAG levels were decreased by ~56%, ~53% and ~22%, respectively, after transfection of HepG2 cells with miR-125a. The TG, TC and DAG levels were decreased, ~80%, ~35% and ~16%, respectively, in Hepa1–6 cells in response to miR-125a treatment. Conversely, inhibition of miR-125a up-regulated TG, TC and DAG levels in both cell lines (Fig. 2B, C and D). We also determined the membrane associated protein levels of PKCε, the intracellular target of DAG, which contributes to insulin resistance by inhibiting the insulin-induced phosphorylation level of insulin receptor substrate. We found that membrane PKCε levels were decreased in HepG2 cells and Hepa1–6 cells after transfection with miR-125a (Supplementary Fig. 2A). Likewise, the lipid accumulation in hepatic cells as measured by BODIPY lipid probe staining (D3922, Invitrogen) was blocked by miR-125a and augmented by miR-125a inhibitor (Fig. 2E). Furthermore, insulin-stimulated phosphorylation of IR at and AKT at were significantly elevated in cells transfected with miR-125a mimics (Fig. 2F and G). In line with increased insulin signaling, overexpression of miR-125a suppressed gluconeogenesis, as demonstrated by reduced mRNA expression of *Pepck* and *G6pase* (Fig. 2H). Interestingly, the expression of lipogenic genes such as acetyl-CoA carboxylase 1 (*Acc1*), fatty acid synthase (*Fasn*) and stearoyl-coenzyme A desaturase 1 (*Scd1*) were also downregulated by miR-125a, while the expression of diacylglycerol O-acyltransferase 1 (*Dgat1*) and carnitine palmitoyltransferase 1A (*Cpt1a*) showed no changes with miR-125a treatment (Fig. 2H and Supplementary 2B). The protein levels of ACC1 and FASN were decreased by miR-125a in HepG2 cells, whereas anti-miR-125a showed the opposite effect (Supplementary Fig. 2C). These results suggested that miR-125a was involved in both gluconeogenesis and lipogenesis.

3.3. MiR-125a improves insulin sensitivity and regulates lipid metabolism in vivo

We next investigated the function of miR-125a in vivo by administering 5′ Chol-labeled miR-125a agomir, miR-125a antagomir or negative control ago-miRNA to male C57BL/6J mice via tail-vein injection. qRT-PCR analysis of RNA from mouse livers demonstrated ~2.5 fold increase of miR-125a in livers of mice that were treated with Ago-miR-125a as compare to negative control ($P < 0.05$). In contrast mice treated with Antago-miR-125a exhibited ~50% decrease in miR-125a levels ($P < 0.05$, Fig. 3A). The mice body weights showed no differences among these three experimental group (Supplementary Fig. 3). Overexpression of miR-125a significantly ameliorated fasting plasma glucose levels, whereas inhibition of miR-125a levels elevated fasting plasma glucose levels (Fig. 3B). GTT and ITT tests indicated that overexpression of miR-125a improved glucose tolerance and insulin sensitivity compared to WT controls (Fig. 3C and D). In addition, insulin-stimulated phosphorylation of IR, and AKT was also significantly increased in the livers of those mice treated with AgomiR-125a (Fig. 3E). Inhibition of miR-125a expression in mice, however, showed decrease of insulin sensitivity (Fig. 3C–E). Moreover, in the mice with ectopic expression of miR-125a, there is a ~20% and ~23% decrease of hepatic TG and TC levels, respectively, when compared with control ($P < 0.05$). In contrary, inhibition of miR-125a with Antago-miR125a result in elevated hepatic TG and TC levels, ~1.23 fold and ~1.25 fold, respectively ($P < 0.05$) (Fig. 3F). Serum TG levels were down-regulated with miR-125a, while TC levels showed no differences with Ago-miR-125a treatment compared to negative control treatment (Fig. 3G). Inhibition of miR-125a with Antago-miR125a increased serum TG levels as well. The serum insulin levels showed no changes in mice after administration of either Ago-miR-125a or Antago-miR125a (Supplementary Fig. 4). Similarly, the hepatic mRNA levels of *Pepck*, *G6pase*, *Acc1*, *Fasn* and *Scd1* were all downregulated following administration of AgomiR-125a, whereas the expression of *Dgat1* showed no changes with AgomiR-125a (Fig. 3H). Furthermore, the hepatic protein levels of ACC1 and FASN were decreased in the mice treated with Ago-miR-125a, while up-regulated by Antago-miR125a (Fig. 3I).

3.4. Overexpression of miR-125a prevents obesity-induced insulin resistance and lipid accumulation in vivo

In order to investigate whether miR-125a can ameliorate obesity-induced insulin resistance, mice that were fed HFD for eight weeks, treated with Ago–miR-125a or negative control miRNA (Fig. 4A) and subsequently subjected to various metabolic measurements. Analysis of hepatic RNA showed ~2.4 fold increase in miR-125a level after twice injections within 5 days ($P < 0.05$) (Fig. 4B). The Ago-miR-125a treated mice exhibited improved glucose tolerance (Fig. 4C) and insulin sensitivity (Fig. 4D) as compared to control miRNA-treated mice. Furthermore, improved insulin sensitivity was paralleled by increased insulin-stimulated phosphorylation of IR and AKT in the livers of Ago-miR-125a-treated mice, compared with controls (Fig. 4E). Cellular levels of hepatic TG and TC were significantly suppressed in Ago-miR-125a-treated mice (Fig. 4F). Serum TG and TC were downregulated by Ago-miR-125a as well (Fig. 4G). Furthermore, overexpression of miR-125a attenuated HFD feeding-induced increase in the serum levels of alanine aminotransferase (ALT) and aspartate aminotransferase (AST) (Fig. 4H and I). Histological analysis further confirmed attenuation of

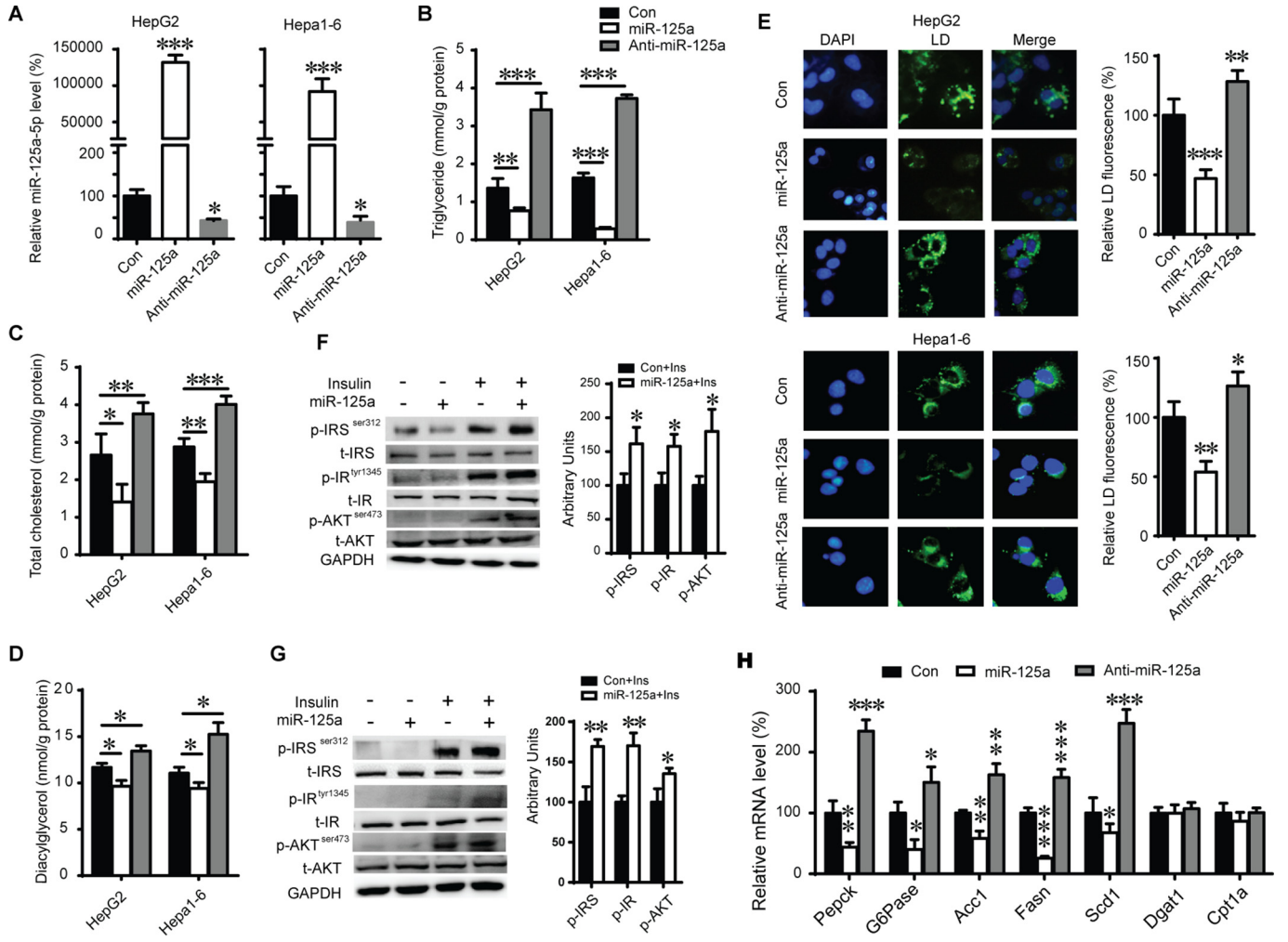

Fig. 2. MiR-125a regulates lipid accumulation and insulin sensitivity in vitro. (A) Relative miR-125a levels in HepG2 cells and Hepa1–6 cells with treatments of miR-125a mimic or miR-125a inhibitor (*P < 0.05; ***P < 0.001; by Mann-Whitney test). (B) TG, (C) TC and (D) DAG levels in HepG2 cells and Hepa1–6 cells with treatments of miR-125a mimic or miR-125a inhibitor (*P < 0.05; **P < 0.01; ***P < 0.001; by Student's *t*-test). (E) Lipid accumulation in HepG2 cells and Hepa1–6 cells labeled with BODIPY lipid probe. Immunoblot analysis of Ser312-phophoylated IRS (p-IRS), total IRS, Tyr1345-phophoylated IR (pIR), total IR, Ser473-phophoylated AKT (p-AKT), and total AKT in HepG2 cells (F) and Hepa1–6 cells (G) transfected with miR-125a and stimulated with insulin (100 nM) for 15 min (*P < 0.05; **P < 0.01; by Student's *t*-test). (H) Relative mRNA levels of *Pepck*, *G6pase*, *Acc1*, *Fasn*, *Scd1*, *Dgat1* and *Cpt1a* in HepG2 cells (*P < 0.05; **P < 0.01; ***P < 0.001; by Student's *t*-test). The results are mean ± SEM (error bars) of triplicate determinations.

obesity-induced lipid accumulation (hepatic steatosis) in Ago-miR-125a-treated mice (Fig. 4J and K). These data strongly suggest that a reduction in miR-125a levels in obese mice contributes to insulin resistance in vivo.

3.5. Identification of ELOVL6 as a target of miR-125a

Using miRNA target prediction tools TargetScan, PicTar and miRanda [37], we investigated the mRNA targets for the miR-125a. The predicted target genes, which are intersectional among three prediction tools, were picked for gene ontology (GO) analysis (Supplementary Table 3), and the genes associated with lipid metabolism and insulin sensitivity were selected for further study (Supplementary Fig. 5). Of the two potential genes (ELOVL6 and QKI) that matched the in silico strategy, we focused on *Elovl6*. ELOVL6, a fatty acyl elongase that performs the initial and rate-limiting condensing reaction required for microsomal elongation of long-chain fatty acids, plays an important role in energy metabolism and insulin sensitivity [38–40]. Measurement of the mRNA and protein levels of Elovl6 demonstrated increase in mRNA and protein, respectively, in obese murine livers and correlated well with the decreased levels of miR-125a (Fig. 5A, B and Supplementary Fig. 6). There are two predictive miR-125a binding sites in 3′UTR of *elovl6*. One of the *elovl6* 3′UTR-pairing sites for miR-125a was well conserved among the vertebrates, whereas other site was poorly conserved (Fig. 5C).

In order to investigate whether miR-125a directly binds to *elovl6* 3′UTR and regulate ELOVL6 expression, the following luciferase reporter plasmids were constructed: pMIR-elovl6-3′UTR-S1, pMIR-elovl6-3′UTR-S2, pMIR-elovl6-3′UTR-S1M and pMIR-elovl6-3′UTR-S2M, containing different pairing sites or mutated sites for miR-125a in the *elovl6* 3′UTR, respectively. As shown in Fig. 5D, the luciferase activity of the plasmids with each *elovl6* 3′UTR-pairing site for miR-125a was abrogated by miR-125a; in contrast, the luciferase activity of the empty control vector and mutated cDNA constructs was not affected by miR-125a (Fig. 5D). Correspondingly, when miR-125a was overexpressed in HepG2 cells, there is a ~40% and ~54% decrease in mRNA and protein levels of ELOVL6 (P < 0.05) (Fig. 5E and F). Likewise, in the mouse that were treated with Ago-miR-125a, where ~2.5 fold overexpression of miR-125a in mouse livers was seen, a ~42% and 51% reduction of ELOVL6 mRNA and protein expression was observed, respectively (P < 0.05); while inhibition of miR-125a by Antago-miR-125a augmented ELOVL6 expression (Fig. 5G and H).

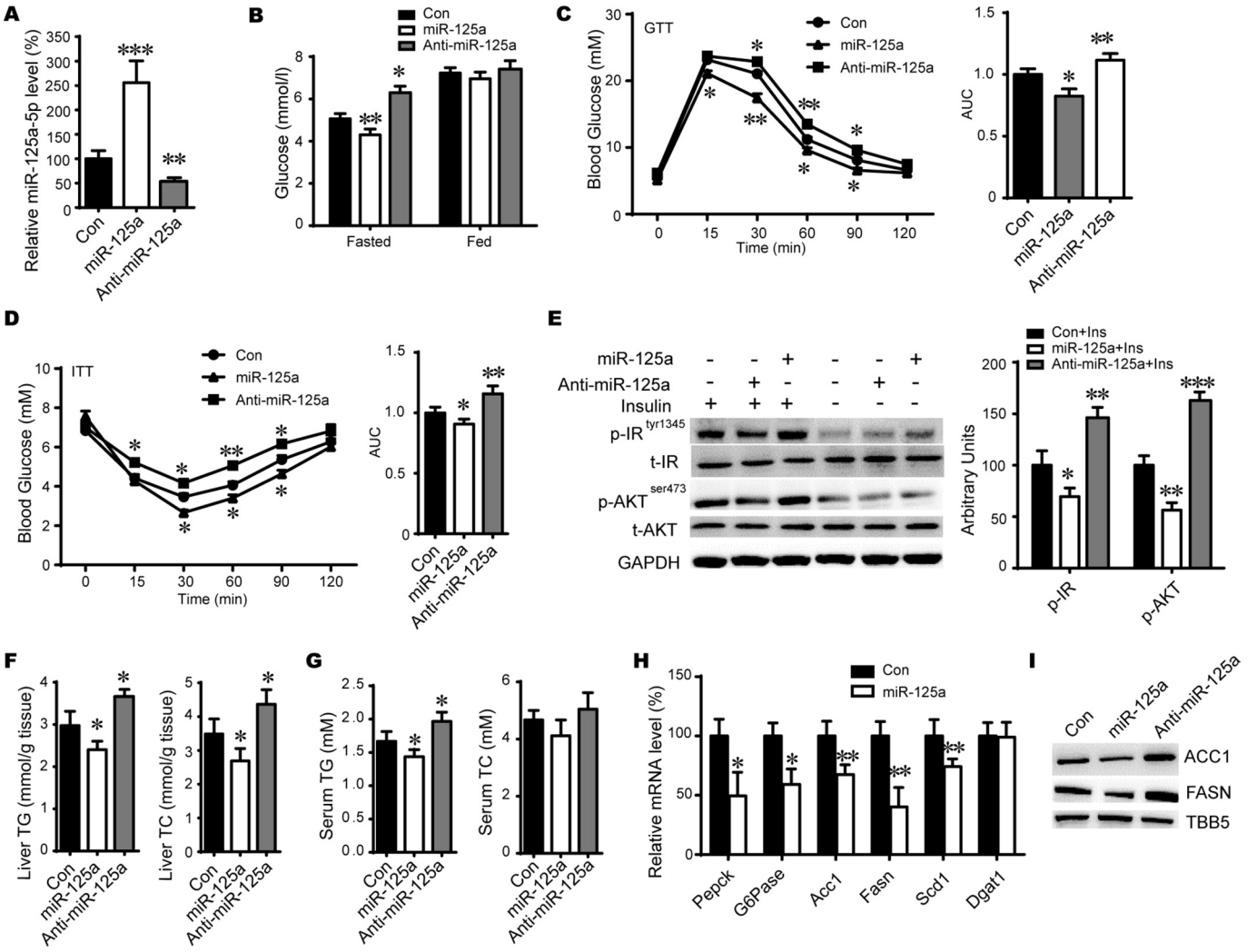

Fig. 3. MiR-125a regulates insulin sensitivity and lipid metabolism in vivo. (A) Relative miR-125a levels in livers of mice injected with ago-miR-125a or antago-miR-125a (**P < 0.01; ***P < 0.001; by Mann-Whitney test). (B) Plasma glucose levels in different treated mice (*P < 0.05; **P < 0.01; by Student's *t*-test). (C, D) GTT (C) and ITT (0.5 U insulin per kg body weight) (D) in mice injected with ago-miR-125a (n = 5), antago-miR-125a (n = 5) or negative control ago-mir (n = 5) (*P < 0.05; **P < 0.01; by Student's *t*-test). For GTT, the mice were fasted for 16 h and then injected with 1 g/kg glucose. For ITT, the mice were fasted for 4 h and injected with 0.5 U/kg insulin and then for blood glucose levels test. (E) Phosphorylation of IR and AKT in the livers of different treated mice (every five mice per group were used, respectively) (*P < 0.05; **P < 0.01; ***P < 0.001; by Student's *t*-test). (F) Liver TG and liver TC levels in the mice injected with ago-miR-125a or antago-miR-125a (*P < 0.05; by Student's *t*-test). Liver tissues were isolated from normal feeding mice treated with/without ago-miR-125a/antago-miR-125a. The liver extracts were used to analyze TC and TG. (G) Serum TG and TC levels in the same mice of F (*P < 0.05; by Student's *t*-test). (H) Relative mRNA levels of *Pepck*, *G6pase*, *Acc1*, *Fasn*, *Scd1* and *Dgat1* in livers of mice overexpressed miR-125a. Liver tissues were isolated like F (*P < 0.05; **P < 0.01; by Student's *t*-test). (I) Protein levels of ACC1 and FASN in the livers of mice as F. The results are mean ± SEM (error bars) of triplicate determinations.

3.6. Overexpression of ELOVL6 impairs the effect of miR-125a on lipid metabolism and insulin sensitivity

To examine the possible involvement of ELOVL6 in miR-125a stimulated-insulin signaling, miR-125a mimics was transduced into HepG2 cells ± overexpression of ELOVL6 (Fig. 6A). As shown in Fig. 6B and C, overexpression of ELOVL6 blocked miR-125a-induced impairments of TG levels and lipid accumulation (P < 0.001). Conversely, overexpression of ELOVL6 attenuated the stimulatory effect of miR-125a on the insulin signaling (Fig. 6D). At the molecular level, overexpression of ELOVL6 relieved miR-125a-induced suppression of gluconeogenic genes expression (*Pepck* and *G6pase*) and lipogenic genes expression (*Acc1*, *Fasn* and *Scd1*) (Fig. 6E). These results indicate that miR-125a regulates insulin signaling and lipid metabolism at least partially through downregulation of ELOVL6 expression.

3.7. MiR-125a modifies fatty acid metabolism in vivo

As summarized above, miR-125a targets and inhibits the expression of ELOVL6, which is involved in the elongation of saturated fatty acids with 12–16 carbons to C18 [39,41]. These data prompted us to further investigate whether miR-125a regulates fatty acid metabolism in vivo. Liver tissues were harvested from mice treated with Ago–miR-125a or negative control miRNA, and hepatic fatty acid compositions were determined by GC/MS (Fig. 7A and B). Consistent with the down-regulation of ELOVL6 in livers of Ago–miR-125a treated mice (Fig. 5G and H), there is decreased hepatic content of stearate (C18:0) and oleate (C18:1n−9), whereas the hepatic content of palmitate (C16:0) and palmitoleate (C16:1n−7) were elevated, as compared to control miRNA treated mice in both chow diet and high-fat diet feeding condition. The ratios of 18:0/16:0 and 16:1/18:1 were consistently decreased and increased, respectively, in the livers of miR-125a treated mice as compared to the control mice (Fig. 7C). These data suggested

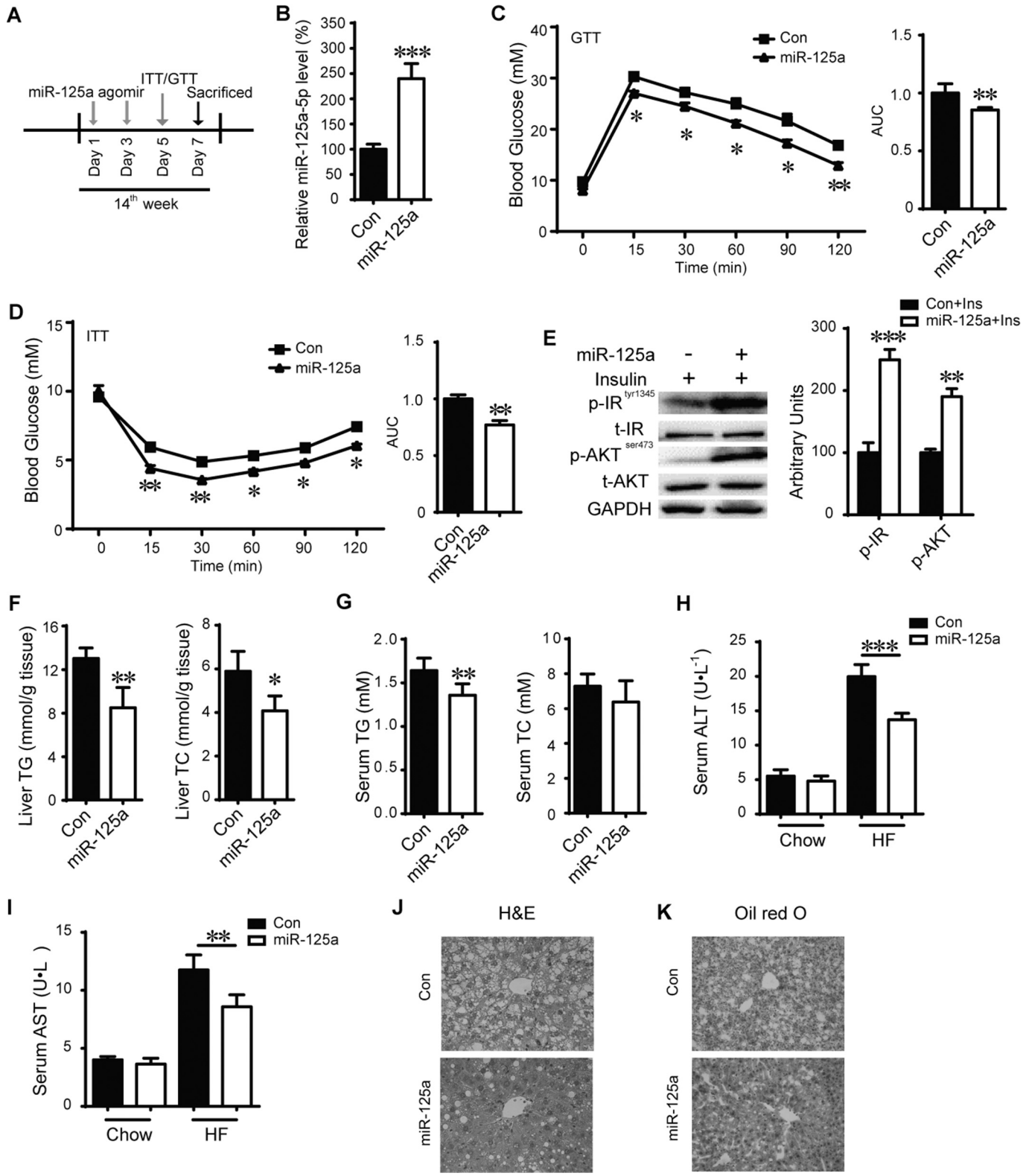

Fig. 4. Overexpression of miR-125a prevents obesity-induced insulin resistance, glucose tolerance, and lipid accumulation. (A) Protocol for Ago–miR-125a delivery. (B) Relative miR-125a levels in the livers of HFD induced obese mice injected with ago-miR-125a (***P < 0.001; by Mann-Whitney test). (C, D) GTT (C) and ITT (D) in DIO mice injected with ago-miR-125a (n = 5) or control ago-mir (n = 5) (*P < 0.05; **P < 0.01; by Student's *t*-test). (E) Phosphorylation of IR and AKT in the livers of different treated DIO mice (every four or five mice per group were used, respectively) (**P < 0.01; ***P < 0.001; by Student's *t*-test). (F) Liver TG and TC in DIO mice (*P < 0.05; **P < 0.01; by Student's *t*-test). For TC and TG test, liver tissues were isolated from HFD feeding mice with/without ago-miR-125a. (G) Serum TG and TC in mice treated as F (*P < 0.05; **P < 0.01; by Student's *t*-test). (H and I) Serum ALT and AST levels in different treated chow-diet feeding mice or DIO mice (**P < 0.01; ***P < 0.001; by Student's *t*-test). (J and K) Representative H&E staining (H) and oil red O staining (I) of paraffin sections from livers of mice fed a HFD and injected with ago-miR-125a or control ago-mir. Data are shown as mean ± SEM (error bars) of triplicate determinations.

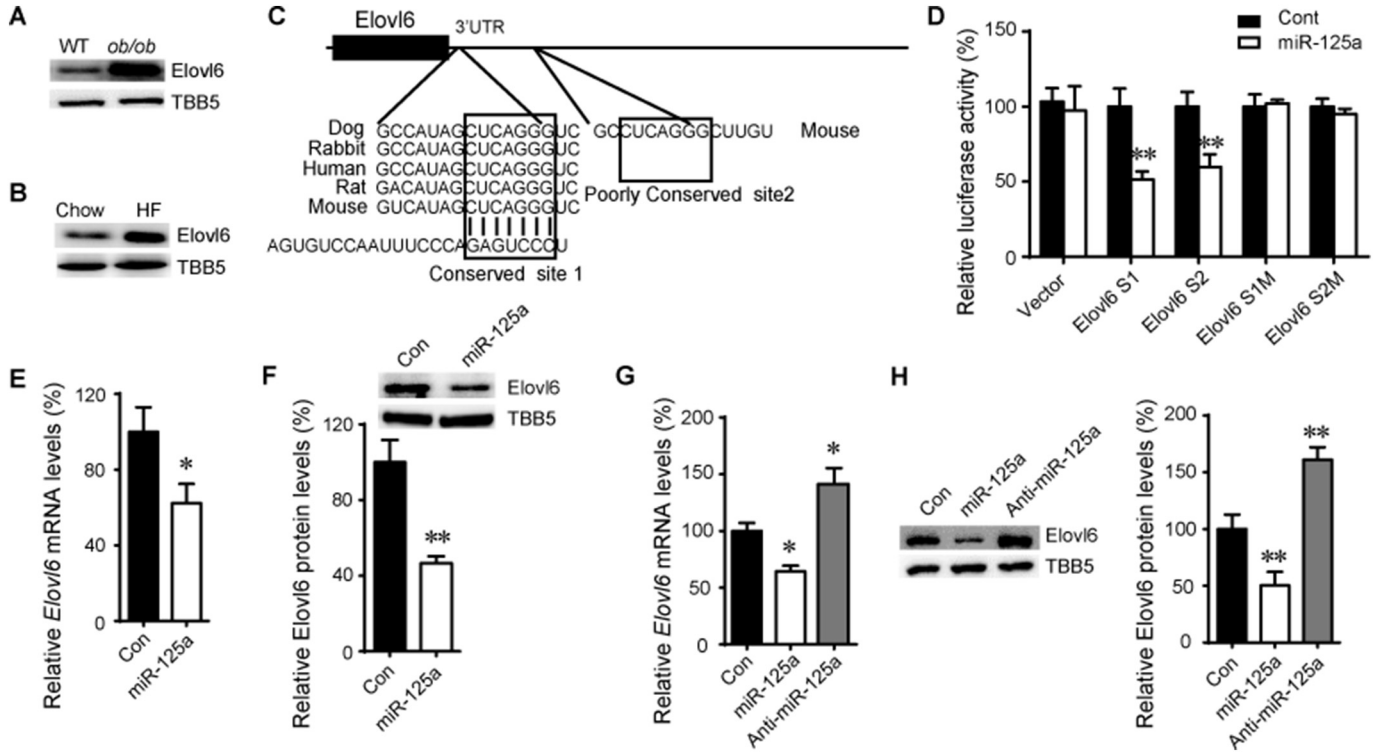

Fig. 5. Identification ELOVL6 as a miR-125a target gene target. The ELOVL6 protein levels was up-regulated in the livers of ob/ob mice (A) and in DIO mice (B). (C) Sequence alignment of miR-125a with 3′UTRs of human (*Homo sapiens*), mouse (*Mus musculus*), Dog (*Canis lupus familiaris*), Rabbit (*Oryctolagus cuniculus*) and rat (*Rattus norvegicus*) ELOVL6. (D) The luciferase activity levels of construct with miR-125a binding sites of ELOVL6 UTR was markedly reduced by miR-125a. The mRNA (E) and protein levels (F) of ELOVL6 were repressed by miR-125a in HepG2 cells. The mRNA levels (G) and protein levels (H) of ELOVL6 in the livers of mice injected with ago-miR-125a, antago-miR-125a or negative control ago-mir. All the data represent the means ± SEM (error bars) of triplicate determinations (*P < 0.05; **P < 0.01; by Student's *t*-test).

that miR-125a regulates hepatic fatty acid metabolism in mice at least in part via attenuation of ELOVL6 mRNA expression.

4. Discussion

Obesity is the most common metabolic disorder in Western societies and during the last few decades, rapidly becoming a major health issue in developing countries including south American and Asian countries. Unhealthy dietary habits with high-calorie, high-fat food consumption are one of the major factors that contribute to obesity epidemic. It is well known that high-fat diet feeding exerts significant modulatory effect on a large number of genes in mouse liver and other tissues [42]. In the present study, we explored the miRNA expression profiles using of mouse livers from chronically fed mice, i.e., high-fat diet-induced obesity mouse model. The expression levels of several miRNAs were significantly altered in DIO mice, and some of them have been implicated in the regulation of lipid metabolism and insulin sensitivity, including miR-143 [19], miR-26a [18], miR-146a [43], miR-103 and miR-107 [20]. Our data indicate that the expression of another miRNA, miR-125a, was markedly repressed in the livers of genetic *ob/ob* and DIO mice.

It is well known that the expression of miR-125a is dysregulated in many kinds of pathological conditions, including tumor [31,44]. Previous studies have reported that the transcription factors, TP53 and PEA3, regulated miR-125a expression by interacting with miR-125a promoter [44,45]. The DNA methylation status of miR-125a promoter also contributes to miR-125a expression [46]. Obesity is associated with chronic, low-grade inflammation, characterized by increased pro-inflammatory cytokine levels, including TNF-α and IL-6 in the circulation and tissues [47]. TNF-α and IL-6 have been reported to regulate expression of several obesity sensitive miRNAs [16,48,49]. We found that the expression of miR-125a levels was markedly attenuated in TNF-α or IL-6 treated HepG2 cells (Supplementary Fig. 7). These data indicate that the expression of miR-125a was regulated by inflammatory cytokines in obese mice.

Others and we have established the role of miR-125a in cell proliferation, carcinogenesis and steroidogenesis [15,26,27]. Our current data uncovered the important functions of miR-125a in the regulation of lipid metabolism and insulin sensitivity. Indeed, we have demonstrated that obesity attenuates miR-125a expression and overexpression of miR-125a significantly improves hepatic steatosis and insulin sensitivity both under in vitro and in vivo conditions. Conversely, inhibition of miR-125a by antago-miR-125a impaired insulin sensitivity and caused elevation of glucose, TG and TC levels. In HFD induced obesity in mice, overexpression of miR-125a ameliorated obesity-induced insulin resistance, glucose tolerance, and lipid accumulation. In line with these metabolic changes, overexpression of miR-125a substantially decreased the mRNA levels of many key genes that regulate lipid and glucose metabolism. These results strongly suggest that reduced miR-125a expression is a primary cause, and not secondarily due to obesity-associated metabolic abnormalities.

Previously, miR-125a was reported to target several downstream proteins that mediate its regulatory functions [27,31]. To determine the molecular basis by which miR-125a regulates insulin sensitivity, we explored other target genes of miR-125a that may be potentially associated with insulin sensitivity. ELOVL6, a microsomal enzyme which catalyzes the elongation of saturated fatty acids (SFA) and monounsaturated fatty acids (MUFA) with 12,14, and 16 carbons, is directly targeted and inhibited by miR-125a. Concomitant with the down-regulation of miR-125a levels, the expression of ELOVL6 is up-regulated in livers of obese mice (Fig. 5). Loss of ELOVL6 function reduces stearate (C18:0) and oleate levels and increases palmitate and palmitoleate

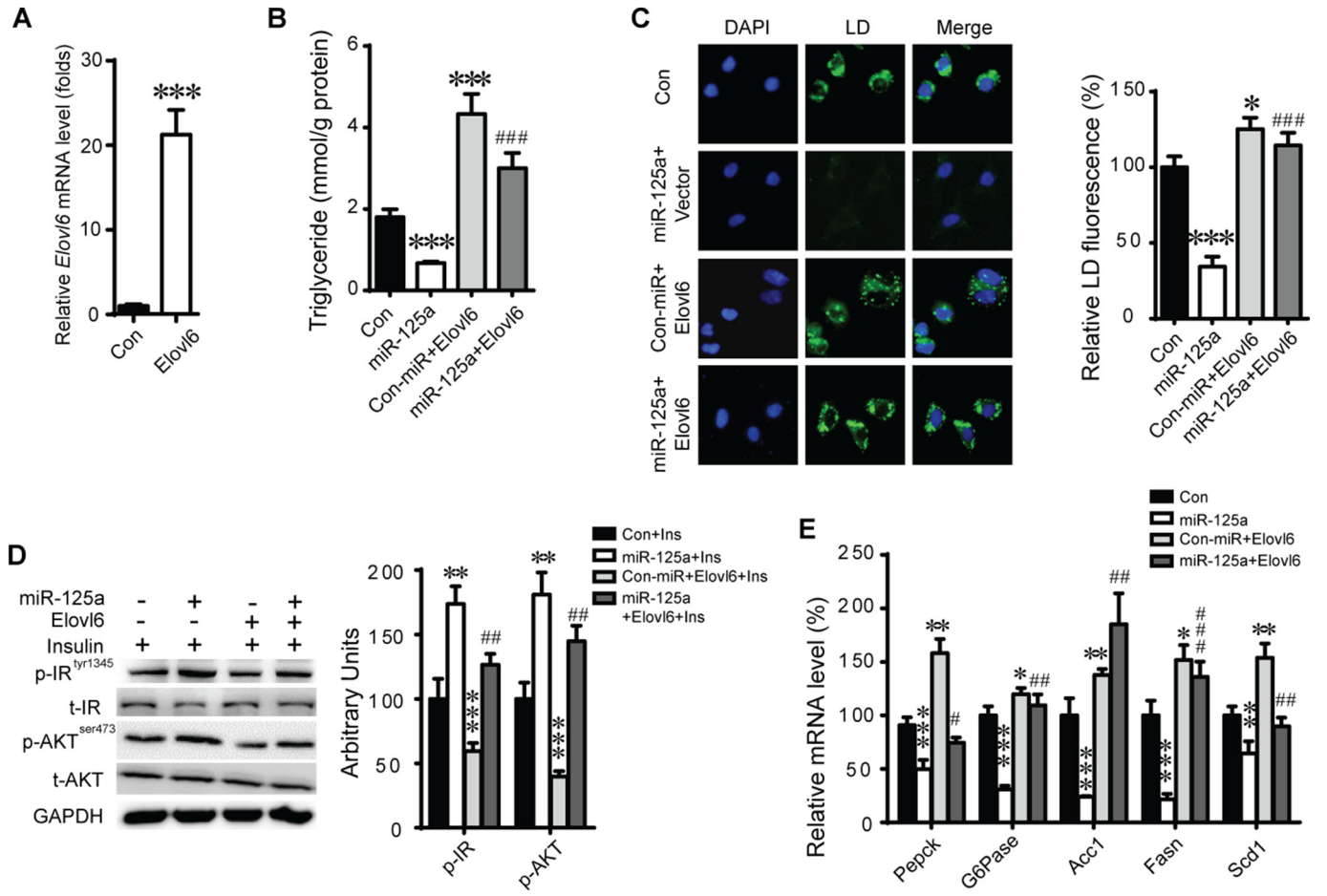

Fig. 6. MiR-125a regulation of lipid metabolism and insulin sensitivity is ELOVL6 dependent. (A) The relative mRNA levels of elovl6 in the HepG2 cells with overexpressed ELOVL6 (***P < 0.001; by Mann-Whitney test). (B) TG levels in HepG2 cells transfected with miR-125a or scrambled nucleotides and ELOVL6 or control vector. (C) Lipid accumulation in different treated HepG2 cells labeled with BODIPY lipid probe. (D) Phosphorylation of IR and AKT in HepG2 cells. (E) Relative mRNA levels of *Pepck*, *G6pase*, *Acc1*, *Fasn* and *Scd1* in HepG2 cells transfected with or without miR-125a mimics and ELOVL6. The data represent the means ± SEM (error bars) of triplicate determinations. (B–C, *P < 0.05, **P < 0.01, ***P < 0.001 vs Control samples; #P < 0.05, ##P < 0.01, ###P < 0.001 vs miR-125a treatment samples; by Student's *t*-test).

levels [50]. We provide evidence that overexpression of miR-125a inhibits ELOVL6 expression, leading to reduction in stearate and oleate levels and increase in palmitate and palmitoleate levels. By regulating hepatic fatty acid composition, ELOVL6 plays a critical role in hepatic steatosis and insulin resistance [38]. We provided evidence that overexpression of miR-125a improved obesity-induce insulin resistance and steatosis in DIO mice. These data indicate that miR-125a directly represses the expression of ELOVL6, which at least partially contribute to the positive effect exerted by miR-125a on insulin signaling. Of note, overexpression of ELOVL6 remarkably restored the miR-125a-inhibited lipid accumulation and interfered with miR-125a-enhanced insulin sensitivity in HepG2 cells.

In addition to ELOVL6, several other metabolic genes that lack predicted miR-125a target sites, showed altered expression in response to modulation of miR-125a expression levels. These enzyme genes are involved in lipid metabolism (*Acc1*, *Fasn*, and *Scd1*), and glucose metabolism/gluconeogenesis (*Pepck*, and *G6pase1*). These data further implicate miR-125a in metabolic homeostasis and insulin sensitivity. Although ELOVL6 deficiency modulated the expression of *Acc1*, *Fasn*, and *Scd1* [38], the exact mechanisms of miR-125a regulation of these genes need explored in the future. Moreover, several other genes have been predicted to be the targets of miR-125a. These genes participated in several different biological pathways (Supplementary Fig. 5). These results implicatemiR-125a in several other novel functions, which will be studied in the future.

In summary, we show that dysregulation miR-125a in obese mice contributes to obesity induced metabolic derangements. Overexpression of miR-125a improves insulin sensitivity and lipid metabolism in vitro and in vivo, via directly targeting ELOVL6. These findings further reveal the critical roles played by miR-125a in the regulation of glucose and lipid metabolism, and insulin signaling, and identify miR-125a as a promising novel target for the development of new treatment strategies in the clinical management of metabolic disorders.

Abbreviations

IR	insulin resistance
T2D	type 2 diabetes
HFD	high-fat diet
Elovl6	ELOVL fatty acid elongase 6
CVD	cardiovascular disease
MetS	metabolic syndrome
NAFLD	nonalcoholic fatty liver disease
miRNAs	microRNAs
SR-B1	scavenger receptor class B, type 1
IR-3T3-L1	insulin resistant 3T3-L1 adipocytes
DIO	diet induced obese
GTT	glucose tolerance test
ITT	insulin tolerance test

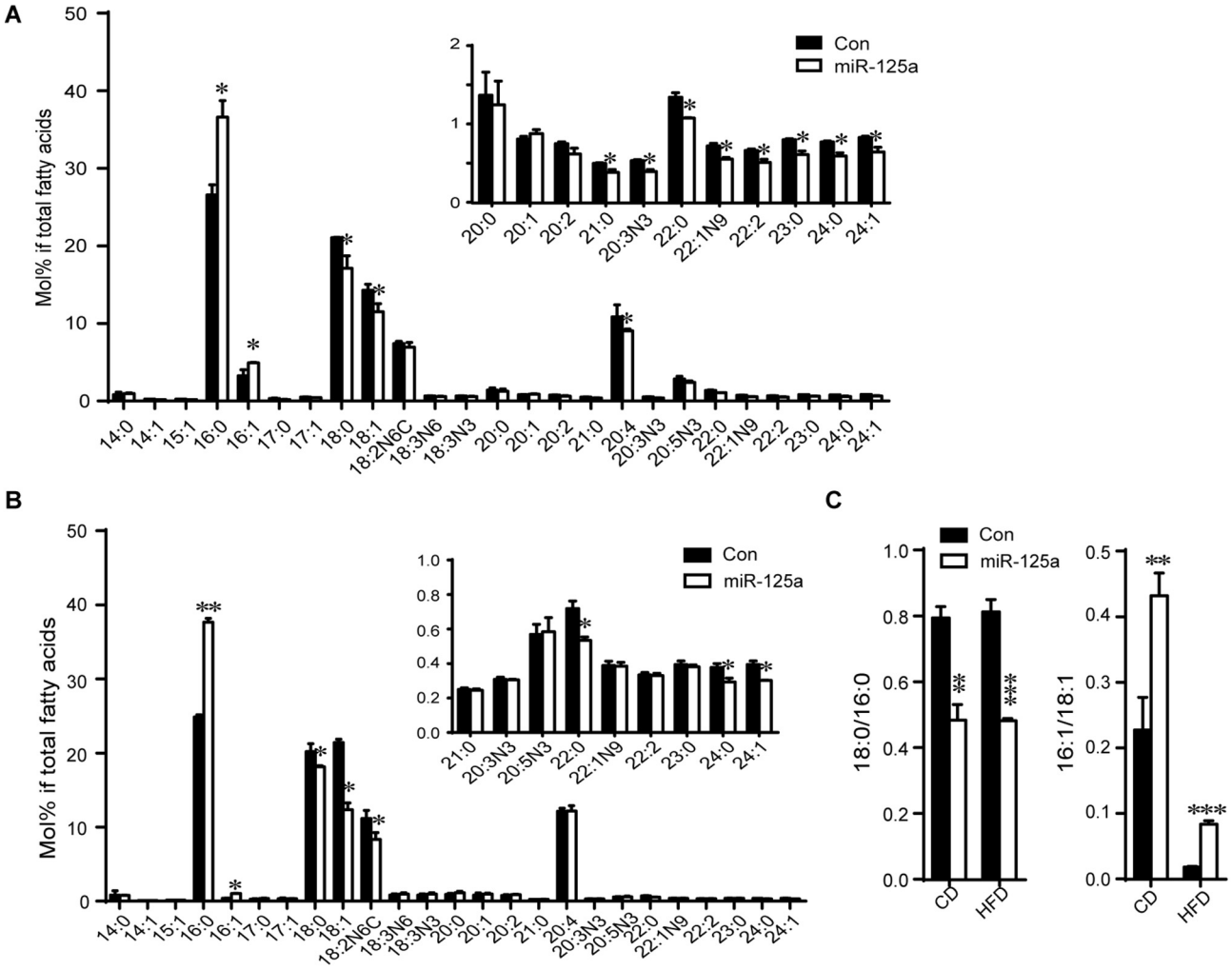

Fig. 7. Overexpression of miR-125a regulates hepatic fatty acid composition. (A, B) Fatty acid composition of liver tissue in mice fed either a normal chow (A) or a HF diet (B) for 8 weeks and then injected with ago-miR-125a (n = 3) or negative control ago-mir (n = 3). (C) The ratio of stearate (18:0) to palmitate (16:0) and palmitoleate (C16:1n−7) to oleate (18:1n−9) in the livers of different mice. All the data represent the means ± SEM (error bars) of triplicate determinations (*P < 0.05; **P < 0.01; ***P < 0.001; by Student's *t*-test).

TG	triglyceride
TC	total cholesterol
GC/MS	gas chromatograph/mass spectrometric
PKC	protein kinase C
Acc1	acetyl-CoA carboxylase 1
Fasn	fatty acid synthase
Scd1	stearoyl-coenzyme a desaturase 1
Dgat1	diacylglycerol O-acyltransferase 1
Cpt1a	carnitine palmitoyltransferase 1A
SFA	saturated fatty acids
MUFA	monounsaturated fatty acids

Funding

This work was supported by National Natural Science Foundation of China (31400659 and 81872284), Natural Science Fund of Colleges and Universities in Jiangsu Province (19KJA180010) and the Priority Academic Program Development of Jiangsu Higher Education Institutions.

Authors' contributions

Conception and design: Z. Hu, Z. Guo; Development of methodology: Z. Hu, R. Liu, M. Wang, Y. Yang, W.J. Shen; Acquisition of data: R. Liu, M. Wang, E. Li, S. Chen, Z. Hu; Analysis and interpretation of data: R. Liu, M. Wang, E. Li, Z. Hu; Drafting the article: R. Liu, W.J. Shen, S. Azhar, Z. Guo, Z. Hu.

Declaration of competing interest

The authors declare that they have no known competing financial interests or personal relationships that could have appeared to influence the work reported in this paper.

Appendix A. Supplementary data

Supplementary data to this article can be found online at https://doi.org/10.1016/j.bbalip.2020.158640.

References

[1] A.R. Saltiel, J.M. Olefsky, Inflammatory mechanisms linking obesity and metabolic disease, J. Clin. Invest. 127 (2017) 1–4.
[2] P. Gonzalez-Muniesa, M.A. Martinez-Gonzalez, F.B. Hu, J.P. Despres, Y. Matsuzawa, R.J.F. Loos, L.A. Moreno, G.A. Bray, J.A. Martinez, Obesity, Nat. Rev. Dis. Primers 3 (2017) 17034.
[3] A. Elagizi, S. Kachur, C.J. Lavie, S. Carbone, A. Pandey, F.B. Ortega, R.V. Milani, An overview and update on obesity and the obesity paradox in cardiovascular diseases,

Prog. Cardiovasc. Dis. 61 (2018) 142–150.
[4] S.A. Gaston, N.S. Tulve, T.F. Ferguson, Abdominal obesity, metabolic dysfunction, and metabolic syndrome in U.S. adolescents: National Health and Nutrition Examination Survey 2011–2016, Annals of Epidemiology 30 (2019) 30–36.
[5] C. Ling, T. Ronn, Epigenetics in human obesity and type 2 diabetes, Cell Metab. 29 (2019) 1028–1044.
[6] S.A. Polyzos, J. Kountouras, C.S. Mantzoros, Obesity and nonalcoholic fatty liver disease: from pathophysiology to therapeutics, Metabolism 92 (2019) 82–97.
[7] S.E. Shoelson, L. Herrero, A. Naaz, Obesity, inflammation, and insulin resistance, Gastroenterology 132 (2007) 2169–2180.
[8] V. Bamba, D.J. Rader, Obesity and atherogenic dyslipidemia, Gastroenterology 132 (2007) 2181–2190.
[9] M.P. Czech, Insulin action and resistance in obesity and type 2 diabetes, Nat. Med. 23 (2017) 804–814.
[10] M.L. Matey-Hernandez, F.M.K. Williams, T. Potter, A.M. Valdes, T.D. Spector, C. Menni, Genetic and microbiome influence on lipid metabolism and dyslipidemia, Physiol. Genomics 50 (2018) 117–126.
[11] M.N. Wang, L.L. Li, R. Liu, Y.W. Song, X.X. Zhang, W.J. Niu, A.K. Kumar, Z.G. Guo, Z.G. Hu, Obesity-induced overexpression of miRNA-24 regulates cholesterol uptake and lipid metabolism by targeting SR-B1, Gene 668 (2018) 196–203.
[12] Z.G. Hu, W.J. Shen, F.B. Kraemer, S. Azhar, Regulation of adrenal and ovarian steroidogenesis by miR-132, J. Mol. Endocrinol. 59 (2017) 269–283.
[13] N. Bushati, S.M. Cohen, microRNA functions, Annu. Rev. Cell Dev. Biol. 23 (2007) 175–205.
[14] M.D. Williams, G.M. Mitchell, MicroRNAs in insulin resistance and obesity, Exp. Diabetes Res. 2012 (2012) 484696.
[15] Z. Hu, W. Shen, F. Kraemer, S. Azhar, MicroRNAs 125a and 455 repress lipoprotein-supported steroidogenesis by targeting scavenger receptor class B type I in steroidogenic cells, Mol. Cell. Biol. 32 (2012) 5035–5045.
[16] Y.M. Yang, S.Y. Seo, T.H. Kim, S.G. Kim, Decrease of microRNA-122 causes hepatic insulin resistance by inducing protein tyrosine phosphatase 1B, which is reversed by licorice flavonoid, Hepatology 56 (2012) 2209–2220.
[17] F. Xiao, J.J. Yu, B. Liu, Y.J. Guo, K. Li, J.L. Deng, J. Zhang, C.X. Wang, S.H. Chen, Y. Du, Y.L. Lu, Y.Z. Xiao, Z. Zhang, F.F. Guo, A novel function of microRNA 130a-3p in hepatic insulin sensitivity and liver steatosis, Diabetes 63 (2014) 2631–2642.
[18] X. Fu, B. Dong, Y. Tian, P. Lefebvre, Z. Meng, X. Wang, F. Pattou, W. Han, X. Wang, F. Lou, R. Jove, B. Staels, D.D. Moore, W. Huang, MicroRNA-26a regulates insulin sensitivity and metabolism of glucose and lipids, J. Clin. Invest. 125 (2015) 2497–2509.
[19] S.D. Jordan, M. Kruger, D.M. Willmes, N. Redemann, F.T. Wunderlich, H.S. Bronneke, C. Merkwirth, H. Kashkar, V.M. Olkkonen, T. Bottger, T. Braun, J. Seibler, J.C. Bruning, Obesity-induced overexpression of miRNA-143 inhibits insulin-stimulated AKT activation and impairs glucose metabolism, Nat. Cell Biol. 13 (2011) 434–446.
[20] M. Trajkovski, J. Hausser, J. Soutschek, B. Bhat, A. Akin, M. Zavolan, M.H. Heim, M. Stoffel, MicroRNAs 103 and 107 regulate insulin sensitivity, Nature 474 (2011) 649–653.
[21] J.W. Kornfeld, C. Baitzel, A.C. Konner, H.T. Nicholls, M.C. Vogt, K. Herrmanns, L. Scheja, C. Haumaitre, A.M. Wolf, U. Knippschild, J. Seibler, S. Cereghini, J. Heeren, M. Stoffel, J.C. Bruning, Obesity-induced overexpression of miR-802 impairs glucose metabolism through silencing of Hnf1b, Nature 494 (2013) 111–115.
[22] N. Nakanishi, Y. Nakagawa, N. Tokushige, N. Aoki, T. Matsuzaka, K. Ishii, N. Yahagi, K. Kobayashi, S. Yatoh, A. Takahashi, H. Suzuki, O. Urayama, N. Yamada, H. Shimano, The up-regulation of microRNA-335 is associated with lipid metabolism in liver and white adipose tissue of genetically obese mice, Biochem. Biophys. Res. Commun. 385 (2009) 492–496.
[23] J.H. Park, J. Ahn, S. Kim, D.Y. Kwon, T.Y. Ha, Murine hepatic miRNAs expression and regulation of gene expression in diet-induced obese mice, Mol. Cells 31 (2011) 33–38.
[24] H.M. Heneghan, N. Miller, O.J. McAnena, T. O'Brien, M.J. Kerin, Differential miRNA expression in omental adipose tissue and in the circulation of obese patients identifies novel metabolic biomarkers, J. Clin. Endocrinol. Metab. 96 (2011) E846–E850.
[25] J.M. Estep, Z. Goodman, H. Sharma, E. Younossi, H. Elarainy, A. Baranova, Z. Younossi, Adipocytokine expression associated with miRNA regulation and diagnosis of NASH in obese patients with NAFLD, Liver Int. 35 (2015) 1367–1372.
[26] N. Potenza, A. Russo, Biogenesis, evolution and functional targets of microRNA-125a, Mol. Gen. Genet. 288 (2013) 381–389.
[27] Y.M. Sun, K.Y. Lin, Y.Q. Chen, Diverse functions of miR-125 family in different cell contexts, J. Hematol. Oncol. 6 (2013) 6.
[28] S. Banerjee, H. Cui, N. Xie, Z. Tan, S. Yang, M. Icyuz, V.J. Thannickal, E. Abraham, G. Liu, miR-125a-5p regulates differential activation of macrophages and inflammation, J. Biol. Chem. 288 (2013) 35428–35436.
[29] G.K. Scott, A. Goga, D. Bhaumik, C.E. Berger, C.S. Sullivan, C.C. Benz, Coordinate suppression of ERBB2 and ERBB3 by enforced expression of micro-RNA miR-125a or miR-125b, J. Biol. Chem. 282 (2007) 1479–1486.
[30] F. Jiang, T. Liu, Y. He, Q. Yan, X. Chen, H. Wang, X. Wan, MiR-125b promotes proliferation and migration of type II endometrial carcinoma cells through targeting TP53INP1 tumor suppressor in vitro and in vivo, BMC Cancer 11 (2011) 425.
[31] N. Coppola, G. de Stefano, M. Panella, L. Onorato, V. Iodice, C. Minichini, N. Mosca, L. Desiato, N. Farella, M. Starace, G. Liorre, N. Potenza, E. Sagnelli, A. Russo, Lowered expression of microRNA-125a-5p in human hepatocellular carcinoma and up-regulation of its oncogenic targets sirtuin-7, matrix metalloproteinase-11, and c-Raf, Oncotarget 8 (2017) 25289–25299.
[32] L. Jiang, Q. Huang, S. Zhang, Q. Zhang, J. Chang, X. Qiu, E. Wang, Hsa-miR-125a-3p and hsa-miR-125a-5p are downregulated in non-small cell lung cancer and have inverse effects on invasion and migration of lung cancer cells, BMC Cancer 10 (2010) 318.
[33] B.M. Herrera, H.E. Lockstone, J.M. Taylor, Q.F. Wills, P.J. Kaisaki, A. Barrett, C. Camps, C. Fernandez, J. Ragoussis, D. Gauguier, M.I. McCarthy, C.M. Lindgren, MicroRNA-125a is over-expressed in insulin target tissues in a spontaneous rat model of Type 2 Diabetes, BMC Med. Genet. 2 (2009) 54.
[34] M.R. Diawara, C. Hue, S.P. Wilder, N. Venteclef, J. Aron-Wisnewsky, J. Scott, K. Clement, D. Gauguier, S. Calderari, Adaptive expression of microRNA-125a in adipose tissue in response to obesity in mice and men, PLoS One 9 (2014) e91375.
[35] X.W. Cui, J.M. Tan, Y.J. Shi, C. Sun, Y. Li, C.B. Ji, J. Wu, Z. Zhang, S.Y. Chen, X.R. Guo, C. Liu, The long non-coding RNA Gm10768 activates hepatic gluconeogenesis by sequestering microRNA-214 in mice, J. Biol. Chem. 293 (2018) 4097–4109.
[36] X. Lu, L. He, Q. Zhou, M. Wang, W.J. Shen, S. Azhar, F. Pan, Z. Guo, Z. Hu, NHERF1 and NHERF2 regulation of SR-B1 stability via ubiquitination and proteasome degradation, Biochem. Biophys. Res. Commun. 490 (2017) 1168–1175.
[37] V. Agarwal, G.W. Bell, J.W. Nam, D.P. Bartel, Predicting effective microRNA target sites in mammalian mRNAs, eLife 4 (2015).
[38] T. Matsuzaka, H. Shimano, N. Yahagi, T. Kato, A. Atsumi, T. Yamamoto, N. Inoue, M. Ishikawa, S. Okada, N. Ishigaki, H. Iwasaki, Y. Iwasaki, T. Karasawa, S. Kumadaki, T. Matsui, M. Sekiya, K. Ohashi, A.H. Hasty, Y. Nakagawa, A. Takahashi, H. Suzuki, S. Yatoh, H. Sone, H. Toyoshima, J. Osuga, N. Yamada, Crucial role of a long-chain fatty acid elongase, Elovl6, in obesity-induced insulin resistance, Nat. Med. 13 (2007) 1193–1202.
[39] T. Matsuzaka, H. Shimano, Elovl6: a new player in fatty acid metabolism and insulin sensitivity, J. Mol. Med. 87 (2009) 379–384.
[40] Y.A. Moon, C.R. Ochoa, M.A. Mitsche, R.E. Hammer, J.D. Horton, Deletion of ELOVL6 blocks the synthesis of oleic acid but does not prevent the development of fatty liver or insulin resistance, J. Lipid Res. 55 (2014) 2597–2605.
[41] A. Jakobsson, R. Westerberg, A. Jacobsson, Fatty acid elongases in mammals: their regulation and roles in metabolism, Prog. Lipid Res. 45 (2006) 237–249.
[42] S. Kim, I. Sohn, J.I. Ahn, K.H. Lee, Y.S. Lee, Y.S. Lee, Hepatic gene expression profiles in a long-term high-fat diet-induced obesity mouse model, Gene 340 (2004) 99–109.
[43] M. Balasubramanyam, S. Aravind, K. Gokulakrishnan, P. Prabu, C. Sathishkumar, H. Ranjani, V. Mohan, Impaired miR-146a expression links subclinical inflammation and insulin resistance in type 2 diabetes, Mol. Cell. Biochem. 351 (2011) 197–205.
[44] Z. Fan, H. Cui, X. Xu, Z. Lin, X. Zhang, L. Kang, B. Han, J. Meng, Z. Yan, X. Yan, S. Jiao, MiR-125a suppresses tumor growth, invasion and metastasis in cervical cancer by targeting STAT3, Oncotarget 6 (2015) 25266–25280.
[45] K.D. Cowden Dahl, R. Dahl, J.N. Kruichak, L.G. Hudson, The epidermal growth factor receptor responsive miR-125a represses mesenchymal morphology in ovarian cancer cells, Neoplasia 11 (2009) 1208–1215.
[46] H. Chen, Z. Xu, Hypermethylation-associated silencing of miR-125a and miR-125b: a potential marker in colorectal cancer, Dis. Markers 2015 (2015) 345080.
[47] P. Dandona, A. Aljada, A. Bandyopadhyay, Inflammation: the link between insulin resistance, obesity and diabetes, Trends Immunol. 25 (2004) 4–7.
[48] C. Shi, L. Zhu, X. Chen, N. Gu, L. Chen, L. Zhu, L. Yang, L. Pang, X. Guo, C. Ji, C. Zhang, IL-6 and TNF-alpha induced obesity-related inflammatory response through transcriptional regulation of miR-146b, J. Interf. Cytokine Res. 34 (2014) 342–348.
[49] N. Zhang, J. Lei, H. Lei, X. Ruan, Q. Liu, Y. Chen, W. Huang, MicroRNA-101 overexpression by IL-6 and TNF-alpha inhibits cholesterol efflux by suppressing ATP-binding cassette transporter A1 expression, Exp. Cell Res. 336 (2015) 33–42.
[50] H. Zhao, T. Matsuzaka, Y. Nakano, K. Motomura, N. Tang, T. Yokoo, Y. Okajima, S.I. Han, Y. Takeuchi, Y. Aita, H. Iwasaki, S. Yatoh, H. Suzuki, M. Sekiya, N. Yahagi, Y. Nakagawa, H. Sone, N. Yamada, H. Shimano, Elovl6 deficiency improves glycemic control in diabetic db/db mice by expanding beta-cell mass and increasing insulin secretory capacity, Diabetes 66 (2017) 1833–1846.